Brain, Behavior, and Immunity 97 (2021) 89–101

Contents lists available at ScienceDirect

Brain Behavior and Immunity

journal homepage: www.elsevier.com/locate/ybrbi

Full-length Article

GluA3 autoantibodies induce alterations in dendritic spine and behavior in mice

Diego Scheggia [a], Jennifer Stanic [a], Maria Italia [a], Filippo La Greca [a], Elisa Zianni [a], Alberto Benussi [b], Barbara Borroni [b], Monica Di Luca [a], Fabrizio Gardoni [a,*]

[a] Department of Pharmacological and Biomolecular Sciences (DiSFeB), University of Milan, 20133 Milan, Italy
[b] Neurology Unit, Centre for Neurodegenerative Disorders, Department of Clinical and Experimental Sciences, University of Brescia, 25123, Brescia, Italy

ARTICLE INFO

Keywords:
Frontotemporal dementia
Encephalitis
Autoimmunity
Glutamate
AMPA receptors
Prefrontal cortex

ABSTRACT

Autoantibodies targeting the GluA3 subunit of AMPA receptors (AMPARs) have been found in patients with Rasmussen's encephalitis and different types of epilepsy and were associated with the presence of learning and attention deficits. Our group recently identified the presence of anti-GluA3 immunoglobulin G (IgG) in about 25% of patients with frontotemporal dementia (FTD), thus suggesting a novel pathogenetic role also in chronic neurodegenerative diseases. However, the *in vivo* behavioral, molecular and morphological effects induced these antibodies are still unexplored. We injected anti-GluA3 IgG purified from the serum of FTD patients, or control IgG, in mice by intracerebroventricular infusion. Biochemical analyses showed a reduction of synaptic levels of GluA3-containing AMPARs in the prefrontal cortex (PFC), and not in the hippocampus. Accordingly, animals injected with anti-GluA3 IgG showed significant changes in recognition memory and impairments in social behavior and in social cognitive functions. As visualized by confocal imaging, functional outcomes were paralleled by profound alterations of dendritic spine morphology in the PFC. All observed behavioral, molecular and morphological alterations were transient and not detected 10–14 days from anti-GluA3 IgG injection. Overall, our *in vivo* preclinical data provide novel insights into autoimmune encephalitis associated with anti-GluA3 IgG and indicate an additional pathological mechanism affecting the excitatory synapses in FTD patients carrying anti-GluA3 IgG that could contribute to clinical symptoms.

1. Introduction

Autoantibodies directed against subunits of ionotropic glutamate receptors have been described in different types of brain disorders, mainly associated with autoimmune encephalitis. The target of these autoantibodies is, in most cases, N-methyl-D-aspartate receptor (NMDAR) (Hunter et al., 2021). However, a growing number of studies identified IgG that recognize subunits of α-amino-3-hydroxy-5-methyl-4-isoxazolepropionic acid receptors (AMPARs) (for review, see Gardoni et al., 2021). In the brain, AMPARs are ligand-gated channels assembled as heterotetrametric receptors mostly composed of GluA1/GluA2 or GluA2/GluA3 subunits (Greger et al., 2017). AMPARs composed by GluA2/GluA3 subunits are enriched at synaptic sites where they are recruited in a constitutive manner replacing GluA1-containing receptors that are inserted at postsynaptic membranes following induction of synaptic plasticity (Jacob and Weinberg, 2015; Shi et al., 2001). IgG against GluA1 and GluA2 have been detected in the cerebrospinal fluid (CSF) of patients with autoimmune encephalitis (Lai et al., 2009; Gleichman et al., 2014). These autoantibodies induced a reversible decrease in the synaptic levels of AMPAR subunits and AMPA-mediated currents without affecting NMDARs, dendritic spine density and cell survival (Lai et al., 2009; Haselmann et al., 2018; Peng et al., 2015). Importantly, *in vivo* administration in mice of anti-GluA2 IgG led to a significative impairment of long-term potentiation and induced recognition memory deficits and anxiety-like behavior (Haselmann et al., 2018). Although anti-GluA3 IgG have been found in patients with Rasmussen's encephalitis and different types of epilepsy (Rogers et al., 1994; Gardoni et al., 2021; Goldberg-Stern et al., 2014) and they have been correlated with the presence of learning and attention problems (Goldberg-Stern et al., 2014), a causal effect of anti-GluA3 IgG in cognitive and behavioral disorders is still unclear.

Our group recently described the presence of IgG that target the GluA3 subunit of AMPAR in about 25% of patients with frontotemporal dementia (FTD) (Borroni et al., 2017; Palese et al., 2020), putting

* Corresponding author.
E-mail address: fabrizio.gardoni@unimi.it (F. Gardoni).

https://doi.org/10.1016/j.bbi.2021.07.001
Received 29 March 2021; Received in revised form 8 June 2021; Accepted 3 July 2021
Available online 9 July 2021

forward the idea of a novel pathogenetic role of these autoantibodies in chronic neurodegenerative diseases (Gardoni et al., 2021). FTD represents a common cause of presenile dementia and a heterogeneous disorder characterized at the onset by behavioral abnormalities, impairment of executive functions and language deficits (Hodges and Piguet, 2018; Seelaar et al., 2011). Administration of anti-GluA3 IgG *in vitro* decreased GluA3 localization in the postsynaptic fraction (Borroni et al., 2017). In agreement, analysis of postmortem specimens from patients carrying anti-GluA3 IgG showed a reduction specifically in GluA3 levels in the frontotemporal cortex, but not in the occipital cortex (Palese et al., 2020). Finally, *in vivo* neurophysiological assessment of excitatory glutamatergic circuits demonstrated a significant reduction in intracortical facilitation in anti-GluA3 positive FTD patients compared to anti-GluA3 negative patients confirming the harmful worsening effect of anti-GluA3 antibodies (Palese et al., 2020). Importantly, these observations are in line with epidemiological, genetic and clinical data, indicating an involvement of the glutamatergic system in FTD (Benussi et al., 2019) as well as an increased risk of autoimmune disorders and autoimmune system dysregulation in FTD patients (Broce et al., 2018; Miller et al., 2016). However, experimental studies to establish *in vivo* a putative role of autoimmunity in the pathogenesis of FTD are still lacking.

In this study, using IgG directed against the GluA3 subunit purified from FTD patients, we show that anti-GluA3 IgG led to distinct changes in cognitive functions and social cognition in mice, and these changes were associated to a reduction of synaptic level of GluA3-containing AMPARs and profound alterations of dendritic spine morphology. Notably, all observed behavioral, molecular and morphological alterations were transient and completely reversed within two weeks from anti-GluA3 IgG intracerebroventricular (ICV) injection. Together, our data represent a step further towards the understanding of the role of anti-GluA3 IgG in FTD pathogenesis.

2. Methods

2.1. Human GluA3 IgG purification

For all participants, informed consent was obtained and sampling protocols were approved by the Ethics Committee of Brescia Hospital, Italy (NP 2939). The study was conducted in accordance with Helsinki Declaration. Affinity purification protocol of the anti-GluA3 IgG from twenty FTD patients' serum was performed by sulfolink affinity chromatography and the human antigenic peptide (GluA3 peptide B, amino acids 399–424). This procedure allowed the acquisition of purified anti-GluA3 IgG at the concentration of 0.12 mg/ml. The same anti-GluA3 IgG purification batch was used for all the experimental procedures.

2.2. Mice

All procedures were approved by the Italian Ministry of Health (permits 441/2020-PR) and local Animal Use Committee and were conducted in accordance with the Guide for the Care and Use of Laboratory Animals of the National Institutes of Health and the European Community Council Directives. Routine veterinary care and animal maintenance was provided by dedicated and trained personnel. A total number of 98 males C57BL/6J animals aged 3 months old were used. Distinct cohorts of naive mice were used for each experiment (behavior, spine morphology, biochemistry; see Fig. 1). Animals were housed two to four per cage in a climate-controlled facility (22 ± 2 °C), with ad libitum access to food and water throughout, and with a 12 h light–dark cycle (19:00–07:00 schedule). Experiments were run during the light phase (within 10:00–17:00). All mice were handled on alternate days during the week preceding the first behavioral testing.

2.3. Surgical procedures

C57BL/6J male mice were anesthetized with a mix of isoflurane (2%) and oxygen (1.5%) by inhalation and mounted into a stereotaxic frame (Kopf Instruments) linked to a digital micromanipulator. Brain coordinates of unilateral intracerebroventricular injection were chosen in accordance with the mouse brain atlas: anterior–posterior (AP), +0.2 mm; medial–lateral (ML): ±1 mm; and dorsal–ventral (DV): −2.5 mm. The volume of anti-GluA3 IgG and control human IgG (R&D Systems, cat. #1-001-A) was 4 µl (0.12 mg/ml). Anti-GluA3 IgG or control IgG, were infused through a 10 µl Hamilton syringe using a microinjection pump at flow rate 1.0 µl/min. Surgical procedure lasted about 20 min for each animal. Mice received carprofen (5 mg/kg) in drinking water for three consecutive days.

2.4. Subcellular fractionation and Western blot (WB) analysis

Triton insoluble postsynaptic fractions (TIF) was isolated from adult mouse prefrontal cortex (PFC) and hippocampus as previously reported (Mellone et al., 2019). To avoid issues related to possible different effects of the Abs in the two hemispheres, left and right PFC and hippocampi were pooled. After measuring protein concentration, all samples were standardized at 1 mg/mL concentration. Acquisition and quantification of WB images were performed by using ChemiDoc™ MP System and Image Lab software (Bio-rad). WB for all tested proteins were normalized against the corresponding tubulin band in the same gel avoiding stripping procedure. This was feasible thanks to horizontal cuts of the membrane considering the higher molecular weight of all AMPAR subunits and scaffolding proteins compared to tubulin. Color broad range pre-stained protein standards were always used (New England Biolabs, #7719). Stripping procedure (RENEW Stripping Buffer, SBS069) was used only to detect CREB, ERK and GluA1 on the same membranes where pCREB, pERK and pGluA1S845 were detected. pCREB, pERK and pGluA1S845 bands were normalized against CREB, ERK and GluA1 bands, respectively. For molecular studies, we analyzed brain samples only from mice that did not undergo behavioral and cognitive tests.

2.5. Spine morphology

Carbocyanine dye DiI (Invitrogen) was used to label neurons as previously reported (Kim et al., 2007; Stanic et al., 2015). Z-stack of 0.45 µm steps were taken with confocal microscope (Zeiss) and analysed using Fiji (ImageJ) software. Specifically, spine length, width and neck

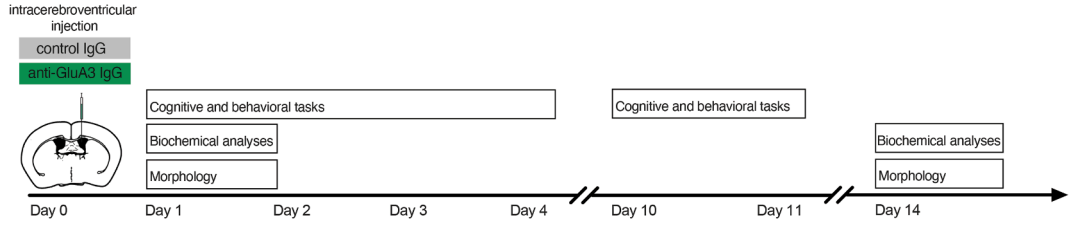

Fig. 1. Scheme representing the timeline of the experimental procedures. Mice were injected with anti-GluA3 IgG or control IgG at 3 months of age. After injection the mice were enrolled in behavioral tests or used for biochemical and morphological experiments.

were manually measured at selected regions of interest. For each dendritic spine, length, head and neck width were measured, which was used to classify dendritic spines into three categories (thin, stubby and mushroom) (see also Harris et al., 1992; Gardoni et al., 2012). In particular, the length and the ratio between the width of head and the width of neck (Wh/Wn) were used as parameters for the classification as follows: protrusions having a length of more than 3 μm were considered as filopodia, the others as spines; spines with a Wh/Wn ratio bigger than 1.7 were considered mushrooms; spines with a Wh/Wn ratio smaller than 1.7 were divided in stubby, if shorter than 1 μm, and thin if longer than 1 μm. Protrusions with length above 3 μm were qualified as filopodia, protrusions with length over 5 μm was excluded from the analysis. For each neuron, an average of 3 basal dendrites, for a total dendritic length of about 200–300 μm, was considered. Basal dendrites, with a distance from the cell body no longer than 300 μm, were analyzed. For spine morphology studies, we analyzed brain samples only from mice that did not undergo behavioral and cognitive tests. To avoid issues related to a possible different effect of the Abs on the two sides, confocal imaging was performed on a balanced number of stained neurons of the two hemispheres.

2.6. Antibodies

The following primary antibodies were used: mouse anti-GluA3 (MAB5416, Millipore, dilution: 1:1000 WB); mouse anti-GluA2 (75–002, Neuromab, dilution: 1:2000 WB); rabbit anti-GluA1 (13185S, Cell Signalling, dilution: 1:1000 WB); rabbit anti-pGluA1^{S845} (3420, Abcam, dilution: 1:1000 WB); mouse anti-PSD95 (192757, Abcam, dilution: 1:2000 WB); rabbit anti-PICK1 (3420, Abcam, dilution: 1:1000 WB); rabbit anti-pERK (9101, Cell Signalling, dilution: 1:1000 WB); rabbit anti-ERK (9102, Cell Signalling, dilution: 1:1000 WB); rabbit anti-pCREB^{S133} (06–519, Millipore, dilution: 1:1000 WB); rabbit anti-CREB (AB3006, Millipore, dilution: 1:1000 WB); mouse anti-Tubulin (T9026, Sigma-Aldrich, dilution: 1:5000 WB). The following secondary antibodies were used: goat anti-mouse-HRP (172–1011, Bio-Rad, dilution: 1:10,000); goat anti-rabbit-HRP (170–6515, Bio-Rad, dilution: 1:10,000).

2.7. Recognition memory tasks

The procedures for novel object recognition, object-in-place and object location tasks were adapted from a previous study (Barker and Warburton, 2011). All the tasks involved an acquisition phase (5 min) and a recognition test (5 min), separated by a 5-minute delay. During the delay period, all the objects were cleaned with alcohol to remove olfactory cues and any sawdust that had stuck to the object. Mice were tested in a standard open field arena (UgoBasile, 44 × 44 cm) with black PVC walls. The stimuli were objects constructed from Duplo blocks (Lego) and varied in shape, color, and size, and were too heavy to be displaced. A digital camera (Imaging Source, DMK 22AUC03 monochrome) was placed above the apparatus to record the test using a behavioral tracking system (Anymaze 6.0, Stoelting). These videos were used offline by experimenters blind to the manipulations for a posteriori scoring of the time spent in the different zones of the apparatus and exploratory behavior, which was defined as the animal directing its nose toward an object at a distance of at least 2 cm. To express the discrimination between the objects we calculated a discrimination ratio as the absolute difference in the time spent exploring the novel, displaced or exchanged objects and the familiar objects divided by the total time spent exploring the objects. All mice were habituated to the open field arena for 15 min the day before testing. Animals that failed to complete a minimum of 10 s of exploration in the test phase were excluded from the analysis. *Novel object recognition task*. Mice were tested in a standard open field arena (UgoBasile, 44 × 44 cm) with black PVC walls. The stimuli were objects constructed from Duplo blocks (Lego) and varied in shape, color, and size, and were too heavy to be displaced. In the acquisition phase, two identical objects were placed near the corners on one wall in the arena (10 cm from the walls). The animals were placed into the arena and allowed to explore for 5 min. During the test, one of the two objects was replaced with a novel object. The positions of the objects in the test and the objects used as novel or familiar were counterbalanced between the animals. *Object location task*. We measured the ability of mice to recognize an object that had changed location compared to the acquisition phase. In the acquisition phase, two identical objects were placed near the corners on one wall in the arena. In the test, one object was left in the same position, the other one was displaced to the corner adjacent to the original position, such that the two objects were diagonal from each other. *Object-in-place task*. In this task four objects were located in the four corners of the arena. In the test phase, two of the objects, both on the left or right of the arena, exchanged positions. If object-in-place memory is intact, the subject should spend more time exploring the two objects that are in different locations compared with the two objects that are in the same locations.

2.8. Fear conditioning

This task was performed as in a previous study (Scheggia et al., 2018). Fear conditioning took place in a standard conditioning chamber (Ugo Basile). The conditioned stimulus (CS) was a tone (4 kHz, 80 dB sound pressure level, 30 s) and the unconditioned stimulus (US) was a scrambled shock (0.7 mA) delivered through the grid floor that terminated simultaneously with the tone (2 s). On experimental day 1, mice were placed in the training chamber and after a 2 min habituation period (baseline) three conditioning trials were presented (tones paired with shock) with an intertrial interval of 90 s. Then, the animals were returned to their home cages 2 min after the last CS–US pairing. After 72 h, mice were retested for long-term memory in the same chamber for 5 min without tone or footshock (contextual memory). At 1 h after the contextual memory recall, mice were placed in a new chamber and after 2 min of habituation (baseline) exposed to the conditioning tone for 2 min (cue) to test cued memory. Then, the animals were returned to their home cages after 2 min (post cue).

2.9. Emotion discrimination task

This task was adapted from previous studies (Ferretti et al., 2019; Scheggia et al., 2020). Testing mice (observers) were tested in a standard three-chamber sociability cage (Ugo Basile, 60x40x22cm) equipped with transparent PVC walls and two grid enclosure that hosted the demonstrators (15 cm in height, diameter 7 cm). After each test, the apparatus was wiped down with 70% ethanol and allowed to air dry. Habituation (10 min) to the testing setting occurred on the day before the first experiment. Both habituation and behavioral testing, were carried under dimly lit (6 ± 1 lx). Digital cameras (Imaging Source, DMK 22AUC03 monochrome) were placed above the apparatus to record the test using a behavioral tracking system (Anymaze 6.0, Stoelting). These videos were used offline by experimenters blind to the manipulations of both the observers and demonstrators for a posteriori scoring of the time spent in the different zones of the apparatus. Animals that failed to complete a minimum of 10 s of exploration were excluded from the analysis.

Demonstrator mice, matched by age, sex, and strain to the observers, were habituated, without the observer, inside the grid enclosure. We counterbalanced the presentation of the neutral versus affectively altered demonstrators in the two sides of the testing arena. *Observers*. Before the test, mice were habituated to the experimental setting and also habituated to the tone cue (4 kHz, 80 dB sound pressure level, once for 120 s) without any conditioning. On the day of testing, 10 min before the experiment, observer mice were gently moved into the dimly lit testing apparatus for habituation. Then, one neutral demonstrator and one emotionally altered demonstrator (fear or stress) mouse were placed under the grid enclosure, and the 6 min experiment started. *Neutral*

demonstrators. All neutral mice were habituated to the experimental setting and to the tone cue as described above. For both fear and stress conditions, neutral demonstrators did not receive any manipulation and were left undisturbed, with ad libitum water access, in their home cage. On the day of testing, neutral demonstrators were brought, inside their home cages, into the experimental room 1 h before the experiment began. All demonstrators were group-housed, separately from the cages of the emotionally altered demonstrators. Demonstrators were test-naive and used a maximum of two times. *Fear demonstrators*. In the days before the test, mice were habituated to the experimental setting as reported above. Fear demonstrators were fear conditioned one day before the test using the parameters and context previously described (Scheggia et al., 2018), and using the same tone delivered to the observers and neutral demonstrators during their habituation process. In particular, the conditioned stimulus was a tone (4 kHz, 80 dB sound pressure level, 30 s) and the unconditioned stimulus were three scrambled shocks (0.7 mA, 2 s duration, 90 s intershock interval) delivered through the grid floor that terminated simultaneously with the tone (2 s). Fear mice were conditioned only once, in a separate room and using distinct apparatus (Ugo Basile, Italy) from the one where the emotion discrimination task would be performed. Fear demonstrators were used only once. *Stress demonstrators*. Mice were subjected to a mild stress consisting of the restraint tube test, a standard procedure to induce physiological stress in rodents for 15 min before the beginning of the test. These mice were then immediately moved to the testing arena.

2.10. Observational fear conditioning

This task was performed as in a previous study (Jeon et al., 2010). The apparatus consisted of two identical and adjacent fear conditioning chambers (Ugo Basile, 24 × 20 × 30 cm) separated by a transparent Plexiglas partition. Olfactory and auditory cues could be transmitted between the chambers. An observer mouse (IgG control or anti-GluA3 IgG) and a sex and age-matched demonstrators were individually placed in the two chamber and allowed to explore the chambers for 5 min (baseline). Then, a 2-s foot shock (0.7 mA) was delivered every 10 s for 4 min to the demonstrator mouse using the behavior tracking software. Demonstrators were used only once. Based on previous studies (Jeon et al., 2010), we used 10-s intervals for foot shocks and a 4-min training. At the end of the procedure demonstrator and observer mice returned to their respective home-cage.

2.11. Sociability and social memory tests

We used the same three-chamber sociability cage employed for the emotion discrimination task. Habituation (10 min) to the testing setting occurred on the day before the experiment. On the day of testing, after habituation in the apparatus without stimuli (10 min), an adult conspecific mouse (novel mouse 1) that had no previous contact with the observer, was placed in the grid enclosure in one side of the apparatus, whereas the other grid enclosure in the opposite chamber was empty. To measure sociability (the tendency of the subject mouse to spend time with a conspecific, compared with time spent with an object), a discrimination ratio was calculated (time spent with novel mouse 1 – time spent with novel object / total time spent with novel mouse 1 and novel object). Following the sociability test, a novel mouse (novel mouse 2) was placed in the empty grid enclosure and the observer was tested for another 5 min to assess the p for social novelty. This is defined as more time spent in the chamber with novel mouse 2 than time in the chamber with novel mouse 1. Most mice prefer to spend more time near the unfamiliar novel mouse (novel mouse 2). To assess social novelty, we calculated a discrimination ratio for each mouse (time spent with novel mouse 2 – time spent with novel mouse 1 / total time spent with novel mouse 1 and novel mouse 2). The procedures and analyses were performed as in previous study (Scheggia et al., 2020).

2.12. Statistical analysis

All the group values are expressed as mean ± s.e.m. Comparisons between groups were performed using the following tests as appropriate: two-tailed unpaired Student's *t* test, Mann–Whitney test or 2-way ANOVA. Statistical analyses were performed using the GraphPad Prism statistical package (GraphPad software). Numbers of neurons and mice used are reported in the figure legends. For Behavioral analysis, data distribution was tested using the D'Agostino and Pearson normality test. The experiments reported in this work were repeated independently two to three times. No statistical methods were used to predetermine sample size for single experiments. The animal numbers were based on estimation from previous studies, including our own published studies (Ferretti et al., 2019; Haselmann et al., 2018; Scheggia et al., 2018, 2020). For all behavioral tests, littermates were randomly assigned to the different groups. Specific randomization in the organization of the experimental design is described in the results and figure legends. Experimenters were not blinded during data acquisition, but all analyses were performed with blinding of the experimental conditions. For molecular/morphological analysis, normal distribution was checked using D'Agostino & Pearson normality test or Shapiro-Wilk normality test. No outliers were identified using ROUT (Q = 1%) method. The raw data that support the findings of this study are available from the corresponding author upon reasonable request.

3. Results

3.1. Injection of antibodies against GluA3 induces molecular and morphological alterations of dendritic spine in the PFC

To evaluate the *in vivo* effects induced by anti-GluA3 IgG purified from FTD patients, male C57BL/6J mice received unilateral stereotaxic cerebroventricular injection of the purified antibody or control IgG (see Fig. 1).

One day after injection, mice were sacrificed and biochemical analyses by WB assay (see Fig. 1) were performed both in a purified triton-insoluble postsynaptic fraction (Mellone et al., 2019) (TIF) and in a total homogenate. As shown in Fig. 2A,B, single injection of anti-GluA3 IgG induced a significant reduction of the GluA3 subunit of AMPARs at synapses of the prefrontal cortex (PFC; Fig. 2A,B) without any modification of the level of this subunit in the total homogenate of the same brain area (Fig. 2C,D). No modifications of the AMPAR GluA1 and GluA2 subunits, of the AMPAR-binding protein PICK1 and of the postsynaptic marker PSD-95 were detected at PFC synapses (Fig. 2A,B) and in PFC homogenate (Fig. 2C,D). Moreover, the phosphorylated form of GluA1 (pGluA1-Ser845; Fig. 2A-D) and the phosphorylated forms of ERK and CREB (Fig. 2E,F) were not altered by the treatment with anti-GluA3 IgG thus suggesting no alteration of the main signaling pathways associated to the activation of synaptic glutamate receptors (Hardingham and Bading, 2010). These same molecular targets were analyzed in TIF (Fig. 2G,H) and total homogenate (data not shown) extracted from mice hippocampus. In this area, single injection of anti-GluA3 IgG did not alter any of the proteins under analysis.

AMPAR activation is a key event in spine enlargement/maturation and formation of new spines (Diering and Huganir, 2018; Hanley, 2008). Previous *in vitro* studies in neuronal cultures demonstrated that treatment with anti-GluA3 IgG induces activation of AMPAR channel (Cohen-Kashi Malina et al., 2006; Levite et al., 1999) and this event is followed by receptor endocytosis (Borroni et al, 2017). However, the role of anti-GluA3 IgG in dendritic spine remodeling *in vivo* was unexplored. Morphological analysis of PFC neurons twenty-four hours after intracerebroventricular injection of anti-GluA3 IgG showed a significant increase in dendritic protrusion density compared with control IgG (Fig. 3A,B). In addition, the anti-GluA3 IgG modified the percentage of spine versus filopodia-like protrusions, leading to a significant increase of filopodia suggesting the ongoing formation of new spines (Fig. 3C,D).

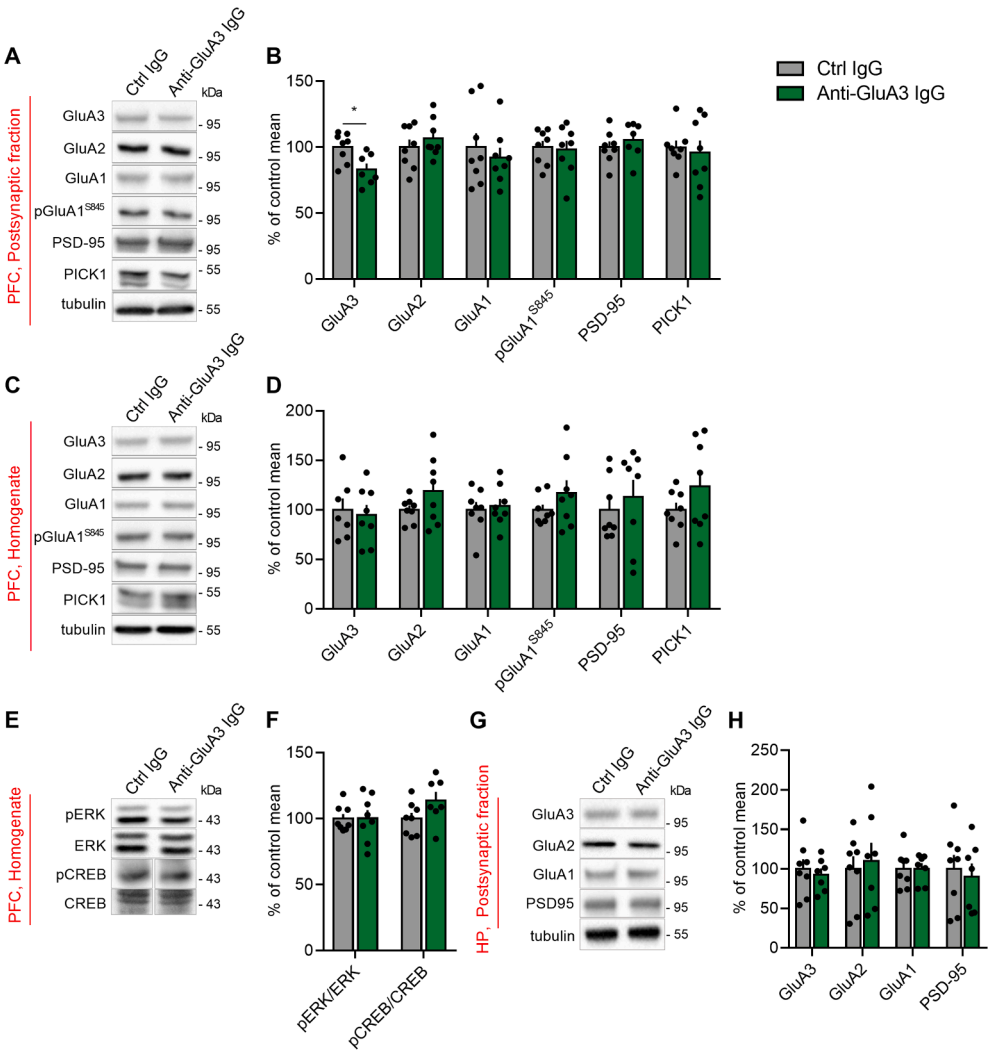

Fig. 2. Molecular effects induced by acute administration of GluA3 IgG in mice. (A-F): Western blot representative images (left panels) and bar graph of densitometric quantification (right panels) of GluA3, GluA2, GluA1 and phosphorylated ser845 GluA1 subunits, PSD-95, PICK, pERK and pCREB in Triton-insoluble postsynaptic fractions (TIF) (A, B) (two-tailed unpaired *t*-test; GluA3: t = 2.861, df = 13, P = 0.0134, n = 7–8/group; GluA2: t = 0.8624, df = 14, P = 0.4030, n = 8/group; GluA1: t = 0.6059, df = 14, P = 0.5543, n = 8/group; PSD95: t = 0.8223, df = 13, P = 0.4258, n = 7–8/group; pGluA1: t = 0.2165, df = 14, P = 0.8317, n = 8/group; PICK1: t = 0.3945, df = 14, P = 0.6992, n = 8/group) and total homogenate (C-F) (two-tailed unpaired *t*-test; GluA3: t = 0.3365, df = 13, P = 0.7419, n = 7–8/group; GluA2: t = 1.476, df = 14, P = 0.1620, n = 8/group; GluA1: t = 0.3512, df = 14, P = 0.7307, n = 8/group; pGluA1: t = 1.248, df = 14, P = 0.2327, n = 8/group; PICK1: t = 1.345, df = 14, P = 0.2001, n = 8/group; pERK: t = 0.03026, df = 14, P = 0.9763, n = 8/group; pCREB: t = 1.803, df = 13, P = 0.0947, n = 7–8/group) (Mann-Whitney test; PSD95: P = 0.4418, n = 8/group) obtained from mice PFC 24 h after injection of either GluA3 IgG or control IgG. (G,H) Western blot representative image (left panel) and densitometric quantification (right panel) of GluA1, GluA2 and GluA3 subunits and PSD-95 in postsynaptic fractions obtained from mice hippocampus 24 h after injection of either anti-GluA3 or control IgG (two-tailed unpaired *t*-test; GluA3: t = 0.4945, df = 13, P = 0.6292, n = 7–8/group; GluA2: t = 0.3572, df = 13, P = 0.7136, n = 7-8group; GluA1: t = 0.0239, df = 13, P = 0.9813, n = 7–8/group; PSD95: t = 0.4009 df = 13, P = 0.6950, n = 7–8/group). Tubulin band was used for normalization. pERK and pCREB proteins were normalized against ERK and CREB bands respectively. n = 7–8 animals. All data are presented as mean ± s.e.m. *P < 0.05. To apply two-tailed unpaired *t*-test, normal distribution was checked using Shapiro-Wilk normality test.

For a more detailed morphological analysis, the dendritic spine length, head and neck width were measured allowing for spines categorization according to their shape (mushroom, stubby and thin) using a highly validated classification method (Harris et al., 1992). Interestingly, anti-GluA3 IgG induced a statistically significant increase in spine head width (Fig. 3E) and spine length (Fig. 3F) thus indicating an overall increase in spine size. Accordingly, anti-GluA3 IgG induced a significant modification of spine type, namely an increase of the percentage of mature mushroom spines and thin spines and a concomitant decrease of stubby spines (Fig. 3G).

3.2. *Injection of antibodies against GluA3 induces impairments of cortical-dependent cognitive functions*

To detect whether antibodies against GluA3 produced *in vivo* behavioral and cognitive changes we first tested cortical-dependent cognitive functions. A new cohort of mice have been injected with anti-GluA3 IgG or control IgG through stereotaxic unilateral intracerebroventricular infusion (see Fig. 1 and Fig. 4A). Twenty-four hours after the injection we did not detect any difference between groups in locomotor activity (Fig. 4B), exploration of the center of the arena, which did not suggest anxiety-like behaviors (Fig. 4C) and grooming behavior (Fig. 4D). On the following day we tested the mice on recognition memory abilities, which require mice to judge about whether a stimulus has been previously encountered. Importantly, recognition memory judgements require the functioning of different cortical regions, such as the perirhinal cortex and the PFC (Barker and Warburton, 2011). We tested anti-GluA3 IgG- or control IgG-injected mice in the novel object recognition task, where the relative familiarity of an object is used to judge prior encounter. Both groups of mice were presented with a pair of identical objects (Fig. 4E) and after a 5-minutes delay, one of the two was replaced with a novel object. Whereas control mice spent more time in the zone related to the novel object, compared to the familiar, mice injected with anti-GluA3 IgG did not show any difference in such behavior (Fig. 4F). We also calculated a discrimination ratio, where positive values indicated increased exploration of the novel over the familiar object and we found that mice injected with anti-GluA3 IgG showed a significantly worse performance compared to control group (Fig. 4G). This effect did not depend on total exploration of the objects, which did not change between the two groups of mice (Fig. 4H). We did

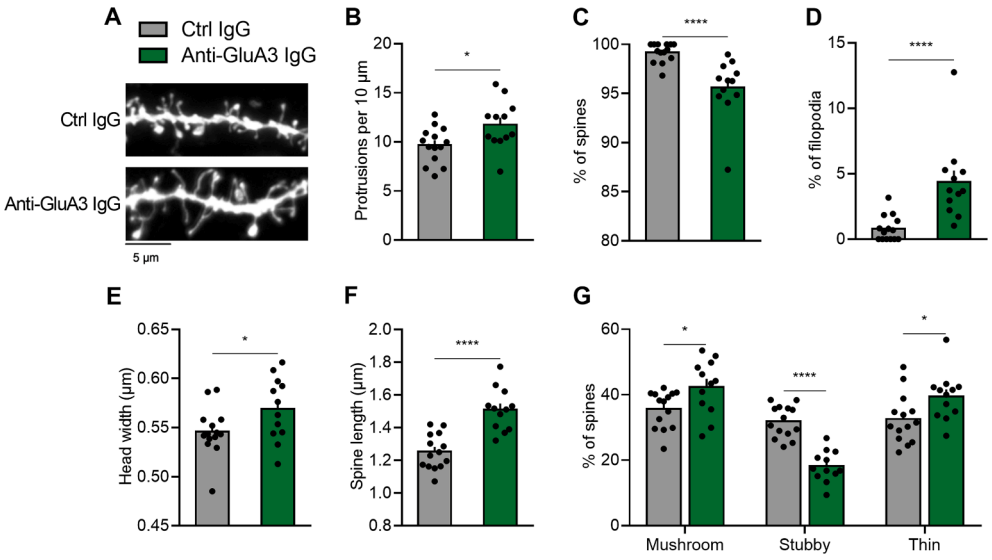

Fig. 3. Effect of acute administration of GluA3 IgG in mice on spine morphology. (A) Representative images showing dendrites of adult mice PFC 24 h after injection of either anti-GluA3 IgG or control IgG (scale bar = 5 µm). (B-G) Bar graphs representing in both conditions (B) protrusion densities (two-tailed unpaired *t*-test, t = 2.523, df = 24, P = 0.0187, n = 12–14 neurons/group), (C) percentages of spines (Mann-Whitney test, P < 0.0001, n = 12–14 neurons/group), (D) percentages of filopodia (Mann–Whitney test, P < 0.0001, n = 12–14/group), (E) spine head width (two-tailed unpaired *t*-test, t = 2.067 df = 24, P = 0.0497, n = 12–14 neurons/group), (F) spine length (two-tailed unpaired *t*-test, t = 5.503, df = 24, P < 0.0001, n = 12–14 neurons/group), (G) proportions of different spine types in percentage of total spines (mushroom, stubby and thin) (two-tailed unpaired *t*-test; mushroom: t = 2.42, df = 24, P = 0.0235; stubby: t = 7.181, df = 24, P < 0.0001; thin: t = 2.368, df = 24, P = 0.0263; n = 12–14 neurons/group). In figures (E) and (F) measurements of width and length referring to different spine types were pooled together; data regarding spine width and length of different spine types compared individually are not showed. All data are presented as mean ± s.e.m. *P < 0.05, ****P < 0.0001. To apply two-tailed unpaired *t*-test, normal distribution was checked using D'Agostino & Pearson normality test.

not observe any difference in the performance compared to non-injected animals (Supplementary Fig. 1). We next tested a different type of recognition memory involving information about where an object has been previously encountered. To do this we used the object-in-place task (Fig. 4I), in which mice were presented with four objects that differed in shape and color, and following a 5-min delay, two of the objects (both in the left or right side of the arena) exchanged position. Also, in this task anti-GluA3 IgG-injected mice failed to show a significant discrimination between the displaced objects and the two that remained in the same position (Fig. 4J,K). We then tested the object location recognition memory (Fig. 4M), which is known to depend more on the functioning of the hippocampus (Barker and Warburton, 2011). In this case we did not observe any difference between anti-GluA3 IgG- and control IgG-injected mice (Fig. 4N,O). These results suggest that injection of the purified anti-GluA3 IgG in mice has an impact on cognitive functions.

In the recognition memory tasks mice were tested after a short delay (5 min) thus to assess whether purified anti-GluA3 IgG could have an impact on long-term memory we used a fear conditioning paradigm that allows the formation of long-lasting memories (Scheggia et al., 2018). Mice were injected with anti-GluA3 IgG or control IgG and then tested in the fear conditioning three days later (Supplementary Fig. 2A). Then, 72 h following the conditioning, mice were re-exposed to the same conditioned context (Supplementary Fig. 2B) and to a novel context (Supplementary Fig. 2C) in which were presented with the conditioned tone (Supplementary Fig. 2D), however, we did not observe any difference as both group of mice displayed similar level of freezing in all these conditions.

3.3. Injection of antibodies against GluA3 induces alteration of social behavior and social cognition

We tested whether injection with antibodies against GluA3 might affect social behavior. Thus, we assessed mice injected with anti-GluA3 IgG or control IgG in a well-validated social approach task (Fig. 5A). Sociability, defined as the tendency of the subject mouse to spend more time with a conspecific, compared with time spent with an inanimate object, was evident in both groups (Fig. 5B). However, this effect was much larger in control IgG-injected mice, thus we calculated a preference score which showed that injection with anti-GluA3 IgG diminished mice social preference versus a conspecific compared to an inanimate object (Fig. 5C). As control we also tested mice social memory, which is their ability to discriminate a familiar conspecific compared to a novel one (Fig. 5D). We did not detect any differences as both groups of mice spent more time in the chamber with the novel mouse than time in the chamber with the familiar mouse (Fig. 5E,F).

We then set out to understand the cause of the different social preference in anti-GluA3 IgG-injected mice. Social cognition and empathy are both regarded as central in social interaction, thus we checked weather these abilities were affected following injection with anti-GluA3 IgG. To test empathy-like behavior in mice we used the observational fear conditioning (Fig. 5G) where empathy occurs by vicariously sensing the emotions of a conspecific (emotional contagion). In this task, an unfamiliar conspecific (demonstrator) and a mouse injected with anti-GluA3 IgG or control IgG (observer) were place in an adjacent compartment, and then the demonstrator received foot shocks (Fig. 5G). We measured freezing behavior, which reflected the observational fear induced by social transmission and we found that mice injected with anti-GluA3 IgG displayed reduced freezing reaction, compared to control IgG-injected mice (Fig. 5H). Both groups of mice spent similar amount of time in exploration of their conspecific demonstrator in the proximity of the divider (Fig. 5I). These results suggested that social transmission and emotional contagion was impaired in anti-GluA3 IgG-injected mice. Further, because this process might depend on social perception and social cognitive processes, we assessed mice abilities to discriminate emotional states in their conspecifics (Scheggia et al., 2020). To test this, mice injected with anti-GluA3 IgG or control IgG tested in the emotion discrimination task where mice were presented with two demonstrator mice, one that underwent fear conditioning ("demonstrator fear"), and the other one that did not receive any manipulation ("demonstrator neutral", Fig. 5J). During the test, mice were presented with the tone cue used for conditioning of the demonstrator fear mouse, and we measured mice preference to spend time with the demonstrators. Whereas control mice spent more time with the emotionally altered demonstrator, mice injected with anti-GluA3 IgG spent similar amount of time with both demonstrators (Fig. 5J and Supplementary Fig. 3). The total number of visits

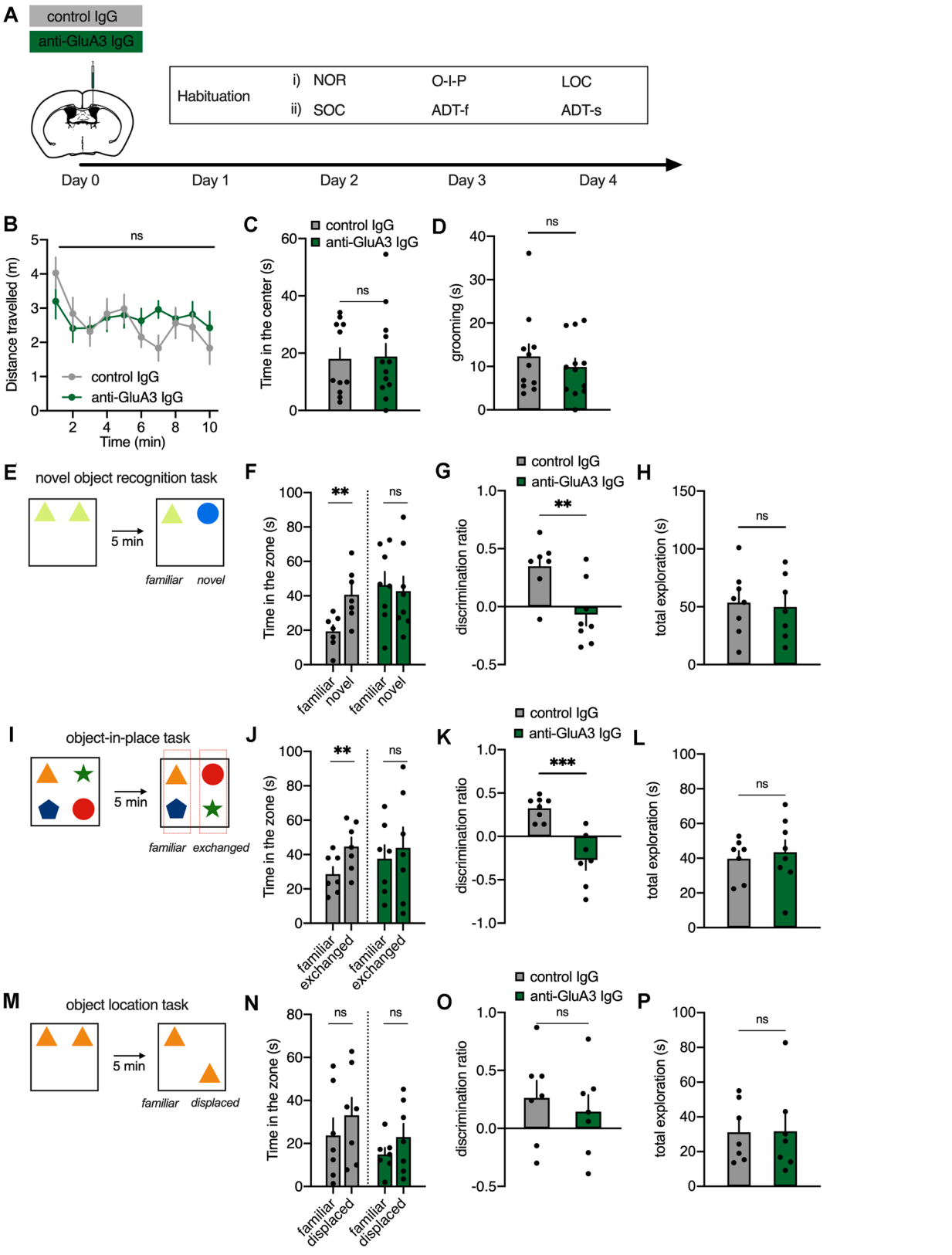

(caption on next page)

Fig. 4. Injection of antibodies against GluA3 induce impairments of cortical-dependent cognitive functions. (A) Experimental design: naïve mice were injected unilaterally in the cerebral ventricle with anti-GluA3 IgG or control IgG and after 24 h tested for behavioral, biochemical or morphological procedures. Mice were assigned to two different groups: i) mice were tested in two of three tasks among novel object recognition (NOR), object-in-place (O-I-P) and object location tasks (LOC). ii) Mice were tested in two of three tasks among social approach (SOC), and emotion discrimination with fear (ADT-f) or stress demonstrators (ADT-s). The order of presentation of these tasks was counterbalanced between mice. The day before testing mice were habituated in the open field arena (i) or the three-chamber arena (ii). (B) Locomotor activity measured as total distance travelled in the open field arena (two-way ANOVA, treatment, $F_{1,21} = 0.11$, P = 0.74). (C) Time spent in the center zone of the open field arena (two-tailed unpaired *t*-test, t = 0.13, df = 21, p = 0.89, n = 11–12/group). (D) Time spent in grooming behavior (two-tailed unpaired *t*-test, t = 0.62, df = 10, P = 0.54, n = 6/group). (E) Schematic of the novel object recognition test. (F) Time spent in the zones related to the familiar or the novel objects (two-tailed multiple *t*-test, Bonferroni correction, control IgG t = 5.58, df = 6, P = 0.002; anti-GluA3 IgG, t = 0.29, df = 7, P = 0.77). (G) Performance of mice injected with anti-GluA3 IgG or control IgG in the novel object recognition task expressed as discrimination ratio (two-tailed unpaired *t*-test, t = 3.15, df = 13, P = 0.0076, n = 7–8/group). (H) Total exploration time (two-tailed unpaired *t*-test, t = 0.04, df = 12, P = 0.38n = 7/group). (I) Schematic of the object-in-place task. (J) Time spent in the zones related to the familiar or the exchanged objects (two-tailed multiple *t*-test, Bonferroni correction, control IgG t = 0.56, df = 6, P = 0.001; anti-GluA3 IgG, t = 0.69, df = 6, P = 0.51). (K) Performance of mice injected with anti-GluA3 IgG or control IgG in the object-in-place task expressed as discrimination ratio (two-tailed unpaired *t*-test, t = 4.92, df = 13, P = 0.0003). (L) Total exploration time (two-tailed multiple *t*-test, Bonferroni correction, control IgG t = 5.58, df = 6, P = 0.002; anti-GluA3 IgG, t = 0.29, df = 7, P = 0.77n = 7–8/group). (M) Schematic of the object location task. (N) Time spent in the zones related to the familiar or the displaced objects (two-tailed multiple *t*-test, Bonferroni correction, control IgG t = 1.04, df = 6, P = 0.33; anti-GluA3 IgG, t = 1.89, df = 6, P = 0.10)). (O) Performance of mice injected with anti-GluA3 IgG or control IgG in the object location task expressed as discrimination ratio (two-tailed unpaired *t*-test, t = 0.57, df = 12, P = 0.52). (P) Total exploration time (two-tailed unpaired *t*-test, t = 0.04, df = 14, P = 0.96, n = 7/group). Bar graphs show mean ± s.e.m. *P < 0.05. **P < 0.01. ***P < 0.0005. n.s., not significant. The performance of all the mice expressed as discrimination ratio fit a normal distribution (D'Agostino and Pearson normality test, n = 44, K2 = 0.92, P = 0.62).

did not differ between the two demonstrators (Supplementary Fig. 3). Furthermore, while the latency to make the first visit towards the demonstrator fear mouse was shorter than towards the neutral demonstrator in the control group (Fig. 5J), anti-GluA3 IgG-injected mice took longer time to explore demonstrator fear mouse. These results suggest that they were not able to make the distinction between the two based on their emotional state. We also tested these mice in a different condition involving a demonstrator mouse subjected to stress ("demonstrator stress", Fig. 5K). However, in this condition, we did not observe any difference between mice injected with anti-GluA3 IgG and control IgG. Also, both group of mice first visited the stressed demonstrator (Fig. 5K). Thus, our results suggested that injection with anti-GluA3 IgG led to significant changes in social transmission and discrimination of emotional states both in relation with affective states of fear.

3.4. Effects mediated by anti-GluA3 IgG injection are transient

To assess whether the observed molecular and behavioral alterations induced by acute intracerebroventricular injection of anti-GluA3 IgG were transient and correlated with anti-GluA3 IgG presence, we repeated the same experiments presented in the previous paragraphs 14 days after anti-GluA3 IgG administration (see Fig. 1). Indeed, 14 days represent a spell of time long enough to ensure the complete wash out of injected IgG from mice brain (Planagumà et al., 2015, 2016).

As shown in Fig. 6A-G, the profound and significant alterations of spine morphology that were present 24 h after anti-GluA3 IgG intracerebroventricular injection, were no longer detectable at day 14. Similarly, WB analysis indicated that anti-GluA3 IgG-injected mice did not differ significantly from control mice in GluA3-containing AMPARs level at synapses of the prefrontal cortex (Fig. 6H,I). These data are in line with our hypothesis of a time-dependent loss of anti-GluA3 IgG effects that accompanies the progressive dilution of this autoantibody and suggests a kind of reversibility of anti-GluA3 IgG-induced alterations.

Similarly, to determine whether a single injection of anti-GluA3 IgG led to transient or permanent effects, mice received anti-GluA3 IgG or control IgG and then were tested 10 days following the injection (see Fig. 1 and Fig. 7A). We first tested mice in the object-in-place, which did not show any difference between the groups as anti-GluA3 IgG-injected mice performed similarly to control IgG mice (Fig. 7B,C). Moreover, we tested mice social behavior, using the three-chamber social approach task that also did not reveal differences between mice injected with anti-GluA3 IgG and control IgG, as both groups of mice similarly spent more time with their conspecific compared to an inanimate object and showed normal social preference (Fig. 7D,E). Thus, these results suggest that behavioral and cognitive effects induced by anti-GluA3 IgG injection were transient and reverted within two weeks after the injection.

4. Discussion

Several studies initially detected anti-GluA3 in the serum of patients with autoimmune encephalitis and in up to 20% to 30% of patients affected by different types of epilepsy (Ganor et al., 2005a, 2005b; Gardoni et al., 2021; Rogers et al., 1994). Interestingly, the presence of anti-GluA3 antibodies correlated with learning, attention and psychiatric symptoms (Goldberg-Stern et al., 2014). More recently, anti-GluA3 IgG have gained further attention in the field of neurology as reports showed that nearly 25% of patients with FTD have autoantibodies that target this AMPAR subunit (Borroni et al., 2017; Palese et al., 2020). Although anti-GluA3 autoantibodies affect glutamatergic neurotransmission *in vitro* through different mechanisms (Borroni et al., 2017; Cisani et al., 2021; Cohen-Kashi Malina et al., 2006; Levite et al., 1999; Palese et al., 2020), the impact of these autoantibodies on cognitive and social functions *in vivo* is still unknown, as well as the biological substrates of these putative modifications. In this study, we demonstrate that a single intracerebral injection of purified anti-GluA3 autoantibodies leads to significant molecular and morphological changes at dendritic spine in the PFC as well as modifications of cognitive and social behavior *in vivo* in mice.

Here we observed that anti-GluA3 IgG affects synaptic levels of the GluA3 subunit in the PFC but not in the hippocampus. Even if AMPARs are widely distributed throughout the brain and represent a key player for activation of the glutamatergic synapse (Hollmann and Heinemann, 1994), their relative abundance varies in the different areas. In particular, hippocampal synapses contains the highest density of AMPARs (Petralia and Wenthold, 1992; Schwenk et al., 2014). Assuming a widespread brain diffusion of ICV injected anti-GluA3 IgG, the increased AMPAR levels in the hippocampus compared to the PFC could account for the observed resilience of hippocampal synaptic AMPAR to molecular modifications induced by the autoantibodies.

Whereas the key role of GluA1 and GluA2 subunits in synaptic plasticity has been well established, the significance of GluA3 still remains not fully addressed. From a functional point of view, GluA2/GluA3 AMPA receptors are recruited in a constitutive manner to synapses, where they can replace GluA1/GluA2 receptors that are usually added to synaptic membranes during synaptic plasticity (Shi et al., 2001). Interestingly, a specific role for GluA2/GluA3 AMPARs in the homeostatic scaling of synaptic strength (Makino and Malinow, 2011) has been put forward, but the lack of GluA3 in hippocampal neurons does impair the induction of synaptic plasticity (Humeau et al., 2007; Reinders et al., 2016). In this line, we detected a significant increase of protrusion density and dendritic spine size in the PFC 24 h after

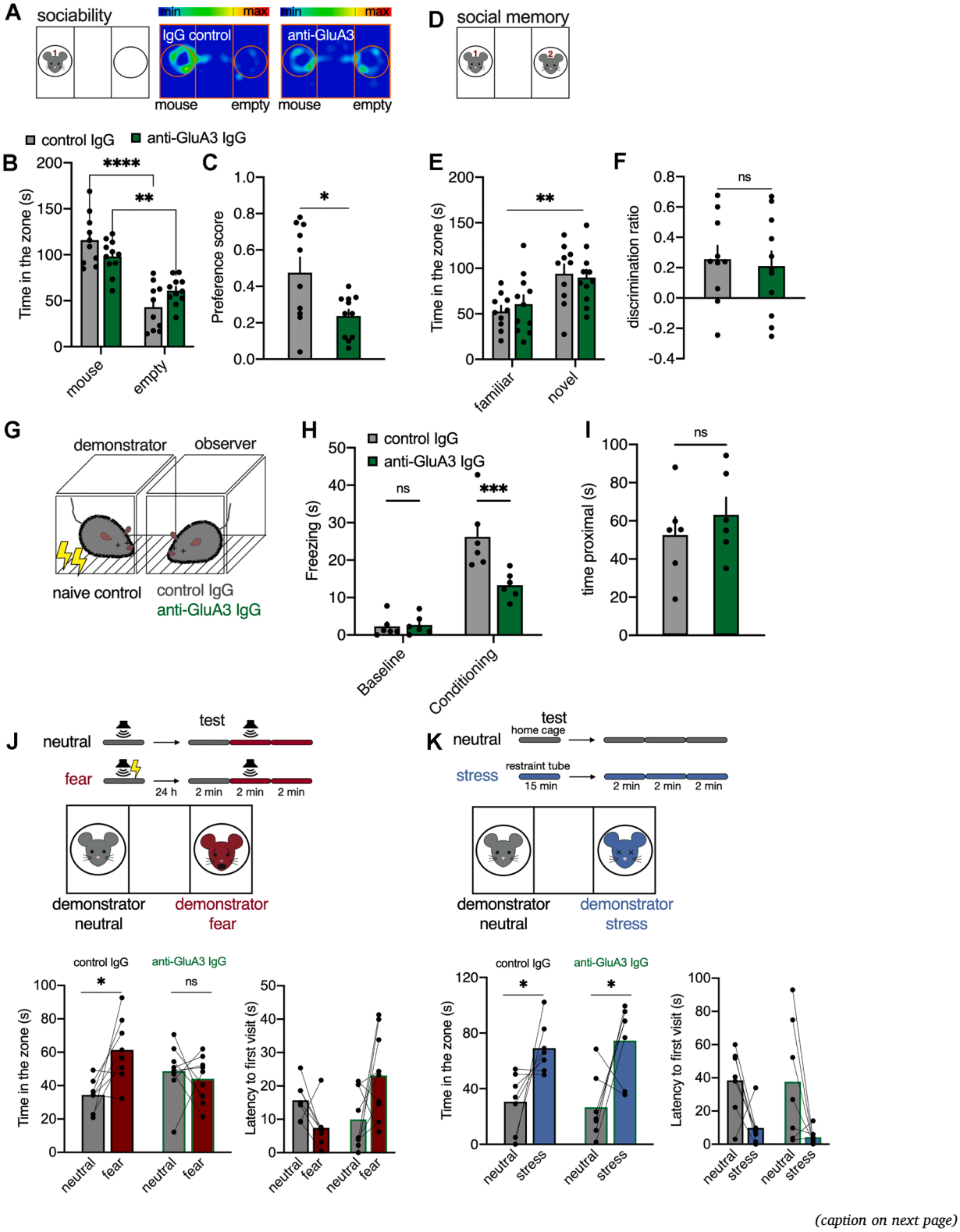

(caption on next page)

Fig. 5. Alteration of social behavior and social cognition after anti-GluA3 IgG injection. (A) Schematic of the social approach task to test sociability in mice injected with anti-GluA3 IgG or control IgG and graphical representation of the amount of time mice spent in different parts of the apparatus (with blue as the shortest and red as the longest time). (B) Time spent by the mice in the chamber with a mouse (mouse 1) or in the empty chamber during the sociability test (two-way ANOVA, group (anti-GluA3 IgG, control IgG) × stimulus (empty, mouse), $F_{1,19} = 7.0$, P = 0.015, n = 10–11/group). (C) Preference to spend time exploring a conspecific compared to an inanimate object measured as preference score (two-tailed unpaired *t*-test, t = 2.68, df = 19, P = 0.01). (D) After sociability, mice were tested for social memory where a novel mouse (mouse 2) was presented in the previously empty chamber. (E) Time spent by the mice in the chamber with the familiar mouse or in the chamber with the novel mouse during the social memory test (two-way ANOVA, stimulus (familiar, novel mouse), $F_{1,19} = 12.84$, P = 0.002, n = 10–11/group). (F) Preference to explore a novel conspecific compared to a familiar one measured as discrimination ratio (two-tailed unpaired *t*-test, t = 0.34, df = 19, P = 0.73). (g) Schematic representation of the observational fear learning. (G) Freezing behavior measured during baseline and conditioning phases of the task in mice injected with anti-GluA3 IgG or control IgG (two-way ANOVA, group (anti-GluA3 IgG, control IgG) × phase (baseline, conditioning), $F_{1,10} = 18.48$, P = 0.0016, n = 6/group). (H) Time spent by the observer in the zone proximal to the demonstrator mouse (two-tailed unpaired *t*-test, t = 0.80, df = 10, P = 0.43). (J,K) Top, Schematic representation of the emotion discrimination task with 'neutral' and 'fear' (J) or 'stress' (K) demonstrators. (J) Bottom, time spent by the mice during the presentation (2-min) of the conditioned tone (two-tailed multiple *t*-test, Bonferroni correction, control IgG t = 3.14, df = 7, P = 0.03; anti-GluA3 IgG, t = 0.55, df = 8, P = 0.59; n = 8–9/group) and latency to make the first visit (two-tailed multiple *t*-test, Bonferroni correction, control IgG t = 2.61, df = 6, P = 0.03; anti-GluA3 IgG, t = 2.63, df = 6, P = 0.03) in the chamber with a neutral demonstrator and in the chamber with fear demonstrator. (K) time spent by the mice during the first 2 min of the task (two-tailed multiple *t*-test, Bonferroni correction, control IgG t = 3.14, df = 7, P = 0.03; anti-GluA3 IgG, t = 0.55, df = 8, P = 0.59; n = 6–7/group) and latency to make the first visit (two-tailed multiple *t*-test, Bonferroni correction, control IgG t = 2.64, df = 6, P = 0.03; anti-GluA3 IgG, t = 2.24, df = 6, P = 0.06) in the chamber with a neutral demonstrator and in the chamber with stress demonstrator Bar graphs show mean ± s.e.m. *P < 0.05. **P < 0.01. ***P < 0.0005. n.s., not significant. Mice scores in the social approach task fit a normal distribution (D'Agostino and Pearson normality test, n = 54, K2 = 0.34, P = 0.84). (For interpretation of the references to color in this figure legend, the reader is referred to the web version of this article.)

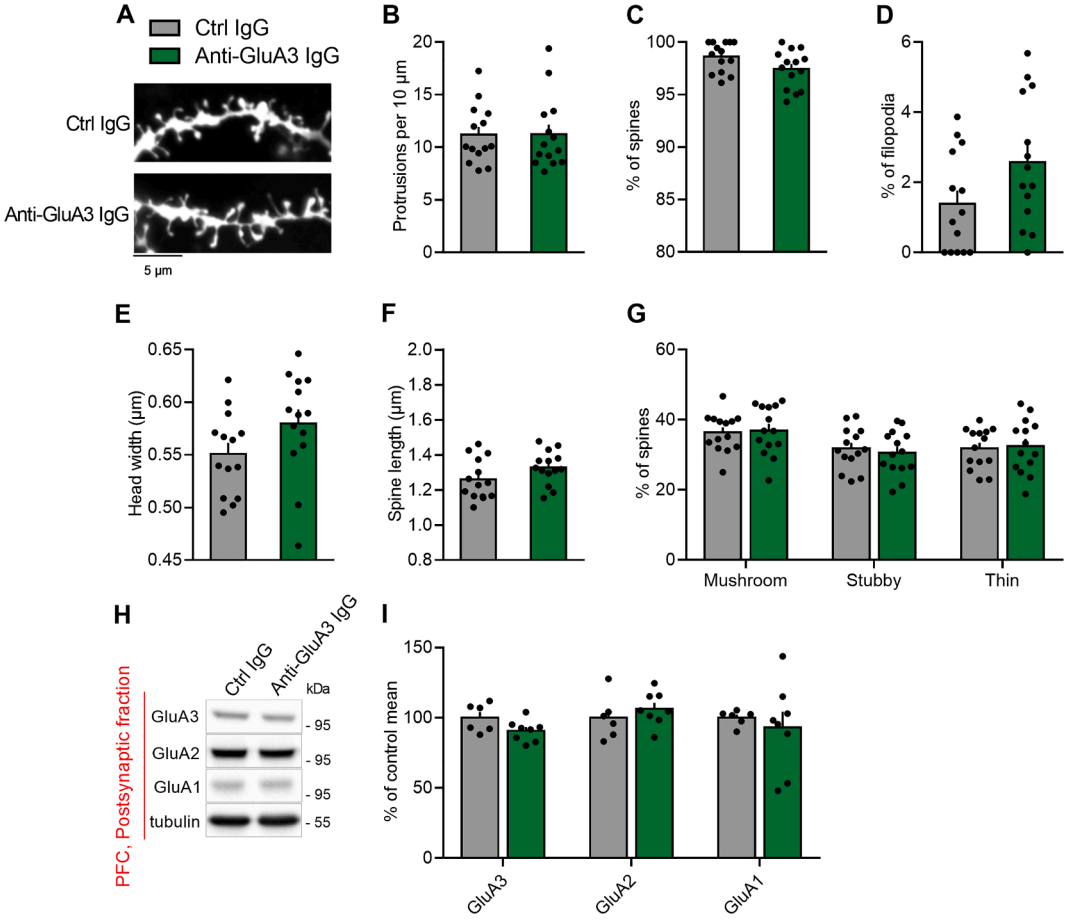

Fig. 6. Molecular and morphological effects in mice of anti-GluA3 IgG are transient. (A) Representative images showing dendrites of adult mice PFC 2 weeks after injection of either anti-GluA3 IgG or control IgG (scale bar = 5 µm). (B-G) Bar graphs representing, in both conditions, (B) the protrusion densities (Mann-Whitney test, P = 0.7345, n = 14/group), (C) percentages of spines (Mann-Whitney test, P = 0.0695, n = 14/group), (D) percentages of filopodia (Mann-Whitney test, P = 0.0695, n = 14/group), (E) spine head width (two-tailed unpaired *t*-test, t = 1.725, df = 26, P = 0.0965, n = 14/group), (F) spine length (two-tailed unpaired *t*-test, t = 1.685, df = 26, P = 0.1040, n = 14/group), (G) proportions of different spine types in percentage of total spines (mushroom, stubby and thin) (two-tailed unpaired *t*-test; mushroom: t = 0.2511, df = 26, P = 0.8037; stubby: t = 0.5266, df = 26, P = 0.6029; thin: t = 0.245, df = 26, P = 0.8083; n = 14/group). (H) Western blot representative image of GluA3, GluA2 and GluA1 subunits in Triton-insoluble postsynaptic fractions (TIF) obtained from mice PFC 2 weeks after injection of either anti-GluA3 IgG or control IgG and (I) corresponding bar graph of densitometric quantification (two-tailed unpaired *t*-test; GluA3: t = 1.985, df = 12, P = 0.0705; GluA2: t = 0.8632 df = 12, P = 0.4049; GluA1: t = 0.5265, df = 12P = 0.6081; n = 6–8/group) . In B-G: n = 14 neurons from 3 animals per condition, in H,I: n = 6–8 animals. All data are presented as mean ± s.e.m. To apply two-tailed unpaired *t*-test, normal distribution was checked using D'Agostino & Pearson normality test or Shapiro-Wilk normality test depending on sample numerosity.

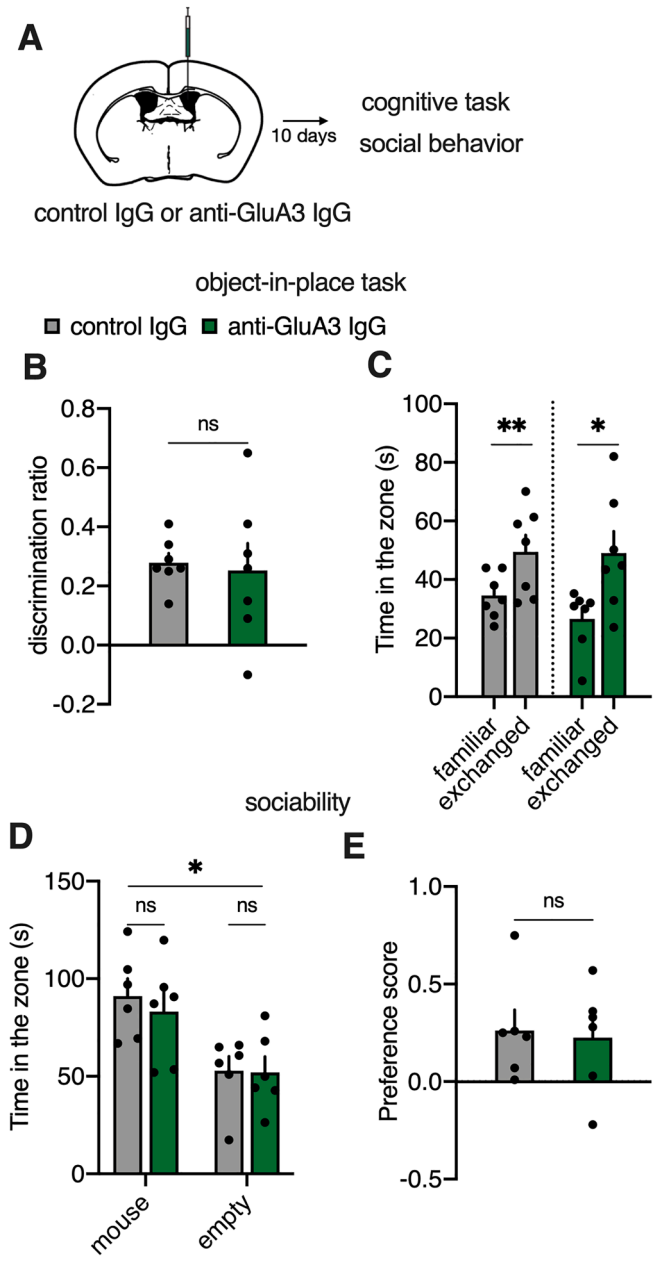

Fig. 7. Effects of anti-GluA3 IgG injection are transient. (A) Experimental design: naïve mice were injected unilaterally in the cerebral ventricle with anti-GluA3 IgG or control IgG and after 10 days cognitive functions and social behavior were assessed. (B) Performance of mice in the object-in-place task expressed as discrimination ratio (two-tailed unpaired *t*-test, t = 0.26, df = 12, P = 0.079, n = 7/group) (C) Time spent in the zones related to the familiar or the exchanged objects (two-tailed multiple *t*-test, Bonferroni correction, control IgG t = 4.68, df = 6, P = 0.006; anti-GluA3 IgG, t = 2.52, df = 6, P = 0.04). (D) Time spent by the mice in the chamber with the mouse or in the empy chamber with the novel mouse during the sociability test (two-way ANOVA, stimulus (familiar, novel mouse), $F_{1,10} = 10.64$, P = 0.008, n = 6/group). (E) Preference to explore a conspecific compared to an inanimate object measured as preference score (two-tailed unpaired *t*-test, t = 0.23, df = 10, P = 0.81). Bar graphs show mean ± s.e.m. *P < 0.05. n.s., not significant.

intracerebral injection of anti-GluA3 IgG. Different explanations can be put forward for this apparently unexpected morphological data. Firstly, previous *in vitro* studies demonstrated that anti-GluA3 IgG can activate GluA3-containing AMPARs (Cohen-Kashi Malina et al., 2006; Levite et al., 1999): this event may lead to a subsequent fast internalization of this pool of AMPARs (Borroni et al., 2017) that are probably replaced by GluA1/GluA2 AMPARs (Shi et al., 2001). Indeed, it is well-know that, following synaptic activation, GluA3-containing AMPARs are physiologically replaced by AMPARs containing GluA1/GluA2 at the post-synaptic membrane. Considering the strict correlation between AMPAR activation, enlargement of pre-existing spines and formation of new ones, antibody-dependent activation can explain the observed morphological alterations.

Our behavioral results showed significant alteration of short-term recognition memory following single injection of anti-GluA3 antibodies. In agreement with previous studies in GluA3-deficient mice we found no effects on spatial (Adamczyk et al., 2012) and contextual memories (Humeau et al., 2007), which are cognitive functions that highly depend on the hippocampus. This is in line also with our molecular findings showing that anti-GluA3 antibodies produced effects in the PFC, while sparing the hippocampus. Indeed, mice injected with anti-GluA3 antibodies displayed marked alterations in cognitive tasks in which the role of the cortex is crucial. The cognitive alterations that we observed particularly involving memory functions could have a translational meaning towards those pathologies in which neuronal antibodies have been shown to impact cognition such as autoimmune encephalitis and FTD. Notably, short-term memory loss and working memory deficits are considered hallmarks of autoimmune encephalitis (Graus et al., 2016) and recognition memory deficits are often observed in FTD patients (Hornberger et al., 2010, 2012). Further, although our data showed alterations of short-memory functions, the impairment on novel object recognition following anti-GluA3 antibodies injection could also indicate problems in the processing of novelty. This could involve a lack of attention to novel stimuli that recall the executive dysfunctions typical of FTD patients (Hornberger et al., 2008). Thus, further research to dissect the exact role of anti-GluA3 antibodies in these cognitive functions is warranted.

In addition to cognitive alterations, we found modifications of social cognitive functions, such as empathy-like behaviors and emotion discrimination, whose processing critically depends on the key role of the PFC (Jeon et al., 2010; Scheggia et al., 2020). Moreover, we expanded previous findings reporting a modulation of social behavior in GluA3-deficient mice (Humeau et al., 2007) by showing that anti-GluA3 antibodies modified social preference. Although our results are in contrast with findings obtained in GluA3-deficient mice they further indicate a possible crucial contribution of GluA3 subunits in social behavior and social cognition. Deficits in theory of mind loss of empathy and emotion processing represent the most prominent symptoms of both autoimmune encephalitis, i.e. limbic encephalitis, and FTD (Henry et al., 2016; Russell et al., 2020; Sprengelmeyer et al., 2010), which clearly have an impact on social daily life of the patients. Here we showed that anti-GluA3 antibodies modified mice social preference and altered social cognitive functions. In particular we found that discrimination of emotional states of fear and social transmission of fear were impaired following anti-GluA3 antibodies injections. These results might suggest that individual differences in empathy-like behaviors and perception of social cues and emotional states might shape social preference. Thus, our results could indicate an important role of an overlooked system involving GluA3-containing AMPAR synaptic transmission in social cognition. Notably, the model we employed in this study, and specifically the immune-neuronal modification of GluA3-containing AMPARs and alterations of dendritic spine morphology, opens up new opportunities for the study and potential treatment of dysfunctional social cognition and particularly emotion processing. Finally, it's worth mentioning that the involvement of the GluA3 subunit in dementia is not limited to FTD but include also Alzheimer's disease (Reinders et al., 2016). Aβ-dependent induction of synaptic dysfunction is strictly correlated to the synaptic removal of GluA3-containing AMPAR and, consequently, GluA3 knockout mice are protected by Aβ-dependent synaptic deficits and memory impairment induced by Aβ (Reinders et al., 2016).

Previous studies related to the *in vivo* infusion in mice of anti-

NMDAR antibodies indicated that all antibody-dependent effects resolved one week after the last administration (Planagumà et al., 2015, 2016). In agreement with these results, here we observed anti-GluA3-dependent effects starting 24 h after injection and leading to behavioral alterations at days 2–4. However, we did not see behavioral, molecular and morphological alterations when experiments were performed 10–14 days after GluA3 injection, thus suggesting that antibody-induced effects at the excitatory glutamatergic synapse are transient and reversible.

In conclusion, even if further studies are needed to evaluate the chronic effect of anti-GluA3 IgG, we can hypothesize that the abnormal presence of anti-GluA3 IgG causing a complex dysfunction in glutamatergic synapses can play a key role in behavioral dysregulation in patients carrying these autoantibodies.

5. Source of funding

This study was supported by Fondazione Umberto Veronesi Young Investigator Grant to DS, and by Min. San. RF-2019-12369272 to MDL.

Declaration of Competing Interest

The authors declare that they have no known competing financial interests or personal relationships that could have appeared to influence the work reported in this paper.

Appendix A. Supplementary data

Supplementary data to this article can be found online at https://doi.org/10.1016/j.bbi.2021.07.001.

References

Adamczyk, A., Mejias, R., Takamiya, K., Yocum, J., Krasnova, I.N., Calderon, J., Cadet, J. L., Huganir, R.L., Pletnikov, M.V., Wang, T., 2012. GluA3-deficiency in mice is associated with increased social and aggressive behavior and elevated dopamine in striatum. Behav. Brain Res. 229, 265–272. https://doi.org/10.1016/j.bbr.2012.01.007.

Barker, G.R., Warburton, E.C., 2011. When is the hippocampus involved in recognition memory? J. Neurosci. 31, 10721–10731. https://doi.org/10.1523/JNEUROSCI.6413-10.2011.

Benussi, A., Alberici, A., Buratti, E., Ghidoni, R., Gardoni, F., Di Luca, M., Padovani, A., Borroni, B., 2019. Toward a glutamate hypothesis of frontotemporal dementia. Front. Neurosci. 13, 304. https://doi.org/10.3389/fnins.2019.00304.

Borroni, B., Stanic, J., Verpelli, C., Mellone, M., Bonomi, E., Alberici, A., Bernasconi, P., Culotta, L., Zianni, E., Archetti, S., Manes, M., Gazzina, S., Ghidoni, R., Benussi, L., Stuani, C., Di Luca, M., Sala, C., Buratti, E., Padovani, A., Gardoni, F., 2017. Anti-AMPA GluA3 antibodies in Frontotemporal dementia: a new molecular target. Sci. Rep. 7, 6723. https://doi.org/10.1038/s41598-017-06117-y.

Broce, I., Karch, C.M., Wen, N., Fan, C.C., Wang, Y., Tan, C.H., Kouri, N., Ross, O.A., Höglinger, G.U., Muller, U., Hardy, J., International FTD-Genomics Consortium., Momeni, P., Hess, C.P., Dillon, W.P., Miller, Z.A., Bonham, L.W., Rabinovici, G.D., Rosen, H.J., Schellenberg, G.D., Franke, A., Karlsen, T.H., Veldink, J.H., Ferrari, R., Yokoyama, J.S., Miller, B.L., Andreassen, O.A., Dale, A.M., Desikan, R.S., Sugrue, L. P., 2018. Immune-related genetic enrichment in frontotemporal dementia: An analysis of genome-wide association studies. PLoS Med. 15, e1002487. 10.1371/journal.pmed.1002487.

Cisani, F., Olivero, G., Usai, C., Van Camp, G., Maccari, S., Morley-Fletcher, S., Pittaluga, A.M., 2021. Antibodies against the NH_2-terminus of the GluA subunits affect the AMPA-evoked releasing activity: the role of complement. Front. Immunol. 12, 586521 https://doi.org/10.3389/fimmu.2021.586521.

Cohen-Kashi Malina, K., Ganor, Y., Levite, M., Teichberg, V.I., 2006. Autoantibodies against an extracellular peptide of the GluR3 subtype of AMPA receptors activate both homomeric and heteromeric AMPA receptor channels. Neurochem. Res. 31, 1181–1190. https://doi.org/10.1007/s11064-006-9143-6.

Diering, G.H., Huganir, R.L., 2018. The AMPA receptor code of synaptic plasticity. Neuron 100, 314–329. https://doi.org/10.1016/j.neuron.2018.10.018.

Ferretti, V., Maltese, F., Contarini, G., Nigro, M., Bonavia, A., Huang, H., Gigliucci, V., Morelli, G., Scheggia, D., Managò, F., Castellani, G., Lefevre, A., Cancedda, L., Chini, B., Grinevich, V., Papaleo, F., 2019. Oxytocin signaling in the central amygdala modulates emotion discrimination in mice. Curr. Biol. 29, 1938–1953.e6. https://doi.org/10.1016/j.cub.2019.04.070.

Ganor, Y., Goldberg-Stern, H., Lerman-Sagie, T., Teichberg, V.I., Levite, M., 2005a. Autoimmune epilepsy: Distinct subpopula-tions of epilepsy patients harbor serum autoantibodies to either glutamate/AMPA receptor GluR3, glutamate/NMDA receptor subunit NR2A or double-stranded DNA. Epilepsy Res. 65, 11–22. https://doi.org/10.1016/j.eplepsyres.2005.03.011.

Ganor, Y., Goldberg-Stern, H., Blank, M., Shoenfeld, Y., Dobrynina, L.A., Kalashnikova, L., Levite, M., 2005b. Antibodies to glutamate receptor subtype 3 (GluR3) are found in some patients suffering from epilepsy as the main disease, but not in patients whose epilepsy accompanies antiphospholipid syndrome or Sneddon's syndrome. Autoimmunity 38, 417–424. https://doi.org/10.1080/08916930500246339.

Gardoni, F., Saraceno, C., Malinverno, M., Marcello, E., Verpelli, C., Sala, C., Di Luca, M., 2012. The neuropeptide PACAP38 induces dendritic spine remodeling through ADAM10-N-cadherin signaling pathway. J. Cell. Sci. 125 (6), 1401–1406. https://doi.org/10.1242/jcs.097576.

Gardoni, F., Stanic, J., Scheggia, D., Benussi, A., Borroni, B., Di Luca, M., 2021. NMDA and AMPA receptor autoantibodies in brain disorders: from molecular mechanisms to clinical features. Cells 10, 77. https://doi.org/10.3390/cells10010077.

Gleichman, A.J., Panzer, J.A., Baumann, B.H., Baumann, B.H., Dalmau, J., Lynch, D.R., 2014. Antigenic and mechanistic characterization of anti-AMPA receptor encephalitis. Ann. Clin. Transl. Neurol. 1, 180–189. https://doi.org/10.1002/acn3.43.

Goldberg-Stern, H., Ganor, Y., Cohen, R., Pollak, L., Teichberg, V., Levite, M., 2014. Glutamate receptor antibodies directed against AMPA receptors subunit 3 peptide B (GluR3B) associate with some cognitive/psychiatric/behavioral abnormali-ties in epilepsy patients. Psychoneuroendocrinol. 40, 221–231. https://doi.org/10.1016/j.psyneuen.2013.11.007.

Graus, F., Titulaer, M.J., Balu, R., Benseler, S., Bien, C.G., Cellucci, T., Cortese, I., Dale, R. C., Gelfand, J.M., Geschwind, M., Glaser, C.A., Honnorat, J., Höftberger, R., Iizuka, T., Irani, S.R., Lancaster, E., Leypoldt, F., Prüss, H., Rae-Grant, A., Reindl, M., Rosenfeld, M.R., Rostásy, K., Saiz, A., Venkatesan, A., Vincent, A., Wandinger, K.P., Waters, P., Dalmau, J., 2016. A clinical approach to diagnosis of autoimmune encephalitis. Lancet Neurol. 15, 391–404. https://doi.org/10.1016/S1474-4422(15)00401-9.

Greger, I.H., Watson, J.F., Cull-Candy, S.G., 2017. Structural and functional architecture of AMPA-type glutamate receptors and their auxiliary proteins. Neuron 94, 713–730. https://doi.org/10.1016/j.neuron.2017.04.009.

Hanley, J.G., 2008. AMPA receptor trafficking pathways and links to dendritic spine morphogenesis. Cell. Adh. Migr. 2, 276–282. https://doi.org/10.4161/cam.2.4.6510.

Hardingham, G.E., Bading, H., 2010. Synaptic versus extrasynaptic NMDA receptor signalling: implications for neurodegenerative disorders. Nat. Rev. Neurosci. 11, 682–696. https://doi.org/10.1038/nrn2911.

Harris, K.M., Jensen, F.E., Tsao, B., 1992. Three-dimensional structure of dendritic spines and synapses in rat hippocampus (CA1) at postnatal day 15 and adult ages: implications for the maturation of synaptic physiology and long-term potentiation. J. Neurosci. 12, 2685–2705. https://doi.org/10.1523/JNEUROSCI.12-07-02685.1992.

Haselmann, H., Mannara, F., Werner, C., Planagumà, J., Miguez-Cabello, F., Schmidl, L., Grünewald, B., Petit-Pedrol, M., Kirmse, K., Classen, J., Demir, F., Klöcker, N., Soto, D., Doose, S., Dalmau, J., Hallermann, S., Geis, C., 2018. Human autoantibodies against the AMPA receptor subunit GluA2 induce receptor reorganization and memory dysfunction. Neuron 100, 91–105. https://doi.org/10.1016/j.neuron.2018.07.048.

Henry, J.D., von Hippel, W., Molenberghs, P., Lee, T., Sachdev, P.S., 2016. Clinical assessment of social cognitive function in neurological disorders. Nat. Rev. Neurol. 12, 28–39. https://doi.org/10.1038/nrneurol.2015.229.

Hodges, J.R., Piguet, O., 2018. Progress and challenges in frontotemporal dementia research: A 20-year review. J. Alzheimer's Dis. 62, 1467–1480. https://doi.org/10.3233/JAD-171087.

Hollmann, M., Heinemann, S., 1994. Cloned glutamate receptors. Annu. Rev. Neurosci. 1994 (17), 31–108. https://doi.org/10.1146/annurev.ne.17.030194.000335.

Hornberger, M., Piguet, O., Kipps, C., Hodges, J.R., 2008. Executive function in progressive and nonprogressive behavioral variant frontotemporal dementia. Neurology 71, 1481–1488. https://doi.org/10.1212/01.wnl.0000334299.72023.c8.

Hornberger, M., Piguet, O., Graham, A.J., Nestor, P.J., Hodges, J.R., 2010. How preserved is episodic memory in behavioral variant frontotemporal dementia? Neurology 74, 472–479. https://doi.org/10.1212/WNL.0b013e3181cef85d.

Hornberger, M., Wong, S., Tan, R., Irish, M., Piguet, O., Kril, J., Hodges, J.R., Halliday, G., 2012. In vivo and post-mortem memory circuit integrity in frontotemporal dementia and Alzheimer's disease. Brain 135, 3015–3025. https://doi.org/10.1093/brain/aws239.

Humeau, Y., Reisel, D., Johnson, A.W., Borchardt, T., Jensen, V., Gebhardt, C., Bosch, V., Gass, P., Bannerman, D.M., Good, M.A., Hvalby, Ø., Sprengel, R., Lüthi, A., 2007. A pathway-specific function for different AMPA receptor subunits in amygdala long-term potentiation and fear conditioning. J. Neurosci. 27, 10947–10956. https://doi.org/10.1523/JNEUROSCI.2603-07.2007.

Hunter, D., Jamet, Z., Groc, L., 2021. Autoimmunity and NMDA receptor in brain disorders: Where do we stand? Neurobiol. Dis. 147, 105161 https://doi.org/10.1016/j.nbd.2020.105161.

Jacob, A.L., Weinberg, R.J., 2015. The organization of AMPA receptor at the postsynaptic membrane. Hippocampus 25, 798–812. https://doi.org/10.1002/hipo.22404.

Jeon, D., Kim, S., Chetana, M., Jo, D., Ruley, H.E., Lin, S.-Y., Rabah, D., Kinet, J.-P., Shin, H.-S., 2010. Observational fear learning involves affective pain system and Cav1.2 Ca2+ channels in ACC. Nat. Neurosci. 13, 482–488. https://doi.org/10.1038/nn.2504.

Kim, B.G., Dai, H.-N., McAtee, M., Vicini, S., Bregman, B.S., 2007. Labeling of dendritic spines with the carbocyanine dye DiI for confocal microscopic imaging in lightly

fixed cortical slices. J. Neurosci. Methods 162, 237–243. https://doi.org/10.1016/j.jneumeth.2007.01.016.

Lai, M., Hughes, E.G., Peng, X., Zhou, L., Gleichman, A.J., Shu, H., Matà, S., Kremens, D., Vitaliani, R., Geschwind, M.D., Bataller, L., Kalb, R.G., Davis, R., Graus, F., Lynch, D. R., Balice-Gordon, R., Dalmau, J., 2009. AMPA receptor Human Autoantibodies in limbic encephalitis alter synaptic receptor location. Ann. Neurol. 65, 424–434. https://doi.org/10.1002/ana.21589.

Levite, M., Fleidervish, I.A., Schwarz, A., Pelled, D., Futerman, A.H., 1999. Autoantibodies to the glutamate receptor kill neurons via activation of the receptor ion channel. J. Autoimmun. 13, 61–67. https://doi.org/10.1006/jaut.1999.0301.

Makino, H., Malinow, R., 2011. Compartmentalized versus global synaptic plasticity on dendrites controlled by experience. Neuron 72, 1001–1011. https://doi.org/10.1016/j.neuron.2011.09.036.

Mellone, M., Zianni, E., Stanic, J., Campanelli, F., Marino, G., Ghiglieri, V., Longhi, A., Thiolat, M.L., Li, Q., Calabresi, P., Bezard, E., Picconi, B., Di Luca, M., Gardoni, F., 2019. NMDA receptor GluN2D subunit participates to levodopa-induced dyskinesia pathophysiology. Neurobiol. Dis. 121, 338–349. https://doi.org/10.1016/j.nbd.2018.09.021.

Miller, Z.A., Sturm, V.E., Camsari, G.B., Karydas, A., Yokoyama, J.S., Grinberg, L.T., Boxer, A.L., Rosen, H.J., Rankin, K.P., Gorno-Tempini, M.L., Coppola, G., Geschwind, D.H., Rademakers, R., Seeley, W.W., Graff-Radford, N.R., Miller, B.L., 2016. Increased prevalence of autoimmune disease within C9 and FTD/MND cohorts: Completing the picture. Neurol. Neuroimmunol. Neuroinflamm. 3, e301 https://doi.org/10.1212/NXI.0000000000000301.

Palese, F., Bonomi, E., Nuzzo, T., Benussi, A., Mellone, M., Zianni, E., Cisani, F., Casamassa, A., Alberici, A., Scheggia, D., Padovani, A., Marcello, E., Di Luca, M., Pittaluga, A., Usiello, A., Borroni, B., Gardoni, F., 2020. Anti-GluA3 antibodies in frontotemporal dementia: effects on glutamatergic neurotransmission and synaptic failure. Neurobiol. Aging 86, 143–155. https://doi.org/10.1016/j.neurobiolaging.2019.10.015.

Peng, X., Hughes, E.G., Moscato, E.H., Parsons, T.D., Dalmau, J., Balice-Gordon, R.J., 2015. Cellular plasticity induced by anti-alpha-amino-3-hydroxy-5-methyl-4-isoxazolepropionic acid (AMPA) receptor encephalitis antibodies. Ann. Neurol. 77, 381–398. https://doi.org/10.1002/ana.24293.

Petralia, R.S., Wenthold, R.J., 1992. Light and electron immunocytochemical localization of AMPA-selective glutamate receptors in the rat brain. J. Comp. Neurol. 318, 329–354. https://doi.org/10.1002/cne.903180309.

Planagumà, J., Leypoldt, F., Mannara, F., Gutiérrez-Cuesta, J., Martín-García, E., Aguilar, E., Titulaer, M.J., Petit-Pedrol, M., Jain, A., Balice-Gordon, R., Lakadamyali, M., Graus, F., Maldonado, R., Dalmau, J., 2015. Human N-methyl D-aspartate receptor antibodies alter memory and behaviour in mice. Brain 138, 94–109. https://doi.org/10.1093/brain/awu310.

Planagumà, J., Haselmann, H., Mannara, F., Petit-Pedrol, M., Grünewald, B., Aguilar, E., Röpke, L., Martín-García, E., Titulaer, M.J., Jercog, P., Graus, F., Maldonado, R., Geis, C., Dalmau, J., 2016. Ephrin-B2 prevents N-methyl-D-aspartate receptor antibody effects on memory and neu-roplasticity. Ann. Neurol. 80, 388–400. https://doi.org/10.1002/ana.24721.

Reinders, N.R., Pao, Y., Renner, M.C., da Silva-Matos, C.M., Lodder, T.R., Malinow, R., Kessels, H.W., 2016. Amyloid-beta effects on synapses and memory require AMPA receptor subunit GluA3. Proc. Natl. Acad. Sci. U.S.A. 113, E6526–E6534. https://doi.org/10.1073/pnas.1614249113.

Rogers, S.W., Andrews, P.I., Gahring, L.C., Whisenand, T., Cauley, K., Crain, B., Hughes, T.E., Heinemann, S.F., McNamara, J.O., 1994. Autoantibodies to glutamate receptor GluR3 in Rasmussen's encephalitis. Science 265, 648–651. https://doi.org/10.1126/science.8036512.

Russell, L.L, Greaves, C.V., Bocchetta, M., Nicholas, J., Convery, R.S., Moore, K., Cash, D. M., van Swieten, J., Jiskoot, L., Moreno, F., Sanchez-Valle, R., Borroni, B., Laforce, R. Jr., Masellis, M., Tartaglia, M.C., Graff, C., Rotondo, E., Galimberti, D., Rowe, J.B., Finger, E., Synofzik, M., Vandenberghe, R., de Mendonça, A., Tagliavini, F., Santana, I., Ducharme, S., Butler, C., Gerhard, A., Levin, J., Danek, A., Otto, M., Warren, J.D., Rohrer, J.D., Genetic FTD Initiative, GENFI., 2020. Social cognition impairment in genetic frontotemporal dementia within the GENFI cohort. Cortex 133, 384-398. 10.1016/j.cortex.2020.08.023.

Scheggia, D., Zamberletti, E., Realini, N., Mereu, M., Contarini, G., Ferretti, V., Managò, F., Margiani, G., Brunoro, R., Rubino, T., De Luca, M.A., Piomelli, D., Parolaro, D., Papaleo, F., 2018. Remote memories are enhanced by COMT activity through dysregulation of the endocannabinoid system in the prefrontal cortex. Mol. Psychiatry 23, 1040–1050. https://doi.org/10.1038/mp.2017.126.

Scheggia, D., Managò, F., Maltese, F., Bruni, S., Nigro, M., Dautan, D., Latuske, P., Contarini, G., Gomez-Gonzalo, M., Requie, L.M., Ferretti, V., Castellani, G., Mauro, D., Bonavia, A., Carmignoto, G., Yizhar, O., Papaleo, F., 2020. Somatostatin interneurons in the prefrontal cortex control affective state discrimination in mice. Nat. Neurosci. 23, 47–60. https://doi.org/10.1038/s41593-019-0551-8.

Schwenk, J., Baehrens, D., Haupt, A., Bildl, W., Boudkkazi, S., Roeper, J., Fakler, B., Schulte, U., 2014. Regional diversity and developmental dynamics of the AMPA-receptor proteome in the mammalian brain. Neuron 84, 41–54. https://doi.org/10.1016/j.neuron.2014.08.044.

Seelaar, H., Rohrer, J.D., Pijnenburg, Y.A., Fox, N.C., van Swieten, J.C., 2011. Clinical, genetic and pathological heterogeneity of frontotemporal dementia: A review. J. Neurol. Neurosurg. Psychiatry 82, 476-486. https://doi.org/ 10.1136/jnnp.2010.212225.

Shi, S., Hayashi, Y., Esteban, J.A., Malinow, R., 2001. Subunit-specific rules governing AMPA receptor trafficking to synapses in hippocampal pyramidal neurons. Cell 105, 331–343. https://doi.org/10.1016/s0092-8674(01)00321-x.

Sprengelmeyer, R., Atkinson, A.P., Sprengelmeyer, A., Mair-Walther, J., Jacobi, C., Wildemann, B., Dittrich, W.H., Hacke, W., 2010. Disgust and fear recognition in paraneoplastic limbic encephalitis. Cortex 46, 650–657. https://doi.org/10.1016/j.cortex.2009.04.007.

Stanic, J., Carta, M., Eberini, I., Pelucchi, S., Marcello, E., Genazzani, A.A., Racca, C., Mulle, C., Di Luca, M., Gardoni, F., 2015. Rabphilin 3A retains NMDA receptors at synaptic sites through interaction with GluN2A/PSD-95 complex. Nat. Commun. 6, 10181. https://doi.org/10.1038/ncomms10181.